Characterizing the contaminant on Chandra ACIS using Abell 1795 observations

Akos Bogdan

for the CXC Calibration group

IACHEC

International Astronomical Consortium for High Energy Calibration

Contaminant on the OBF

- Molecular contaminant on the ACIS optical blocking filter
- Absorption from C, O, F
- Time dependence
- Spatial dependence
- Time dependent chemical composition

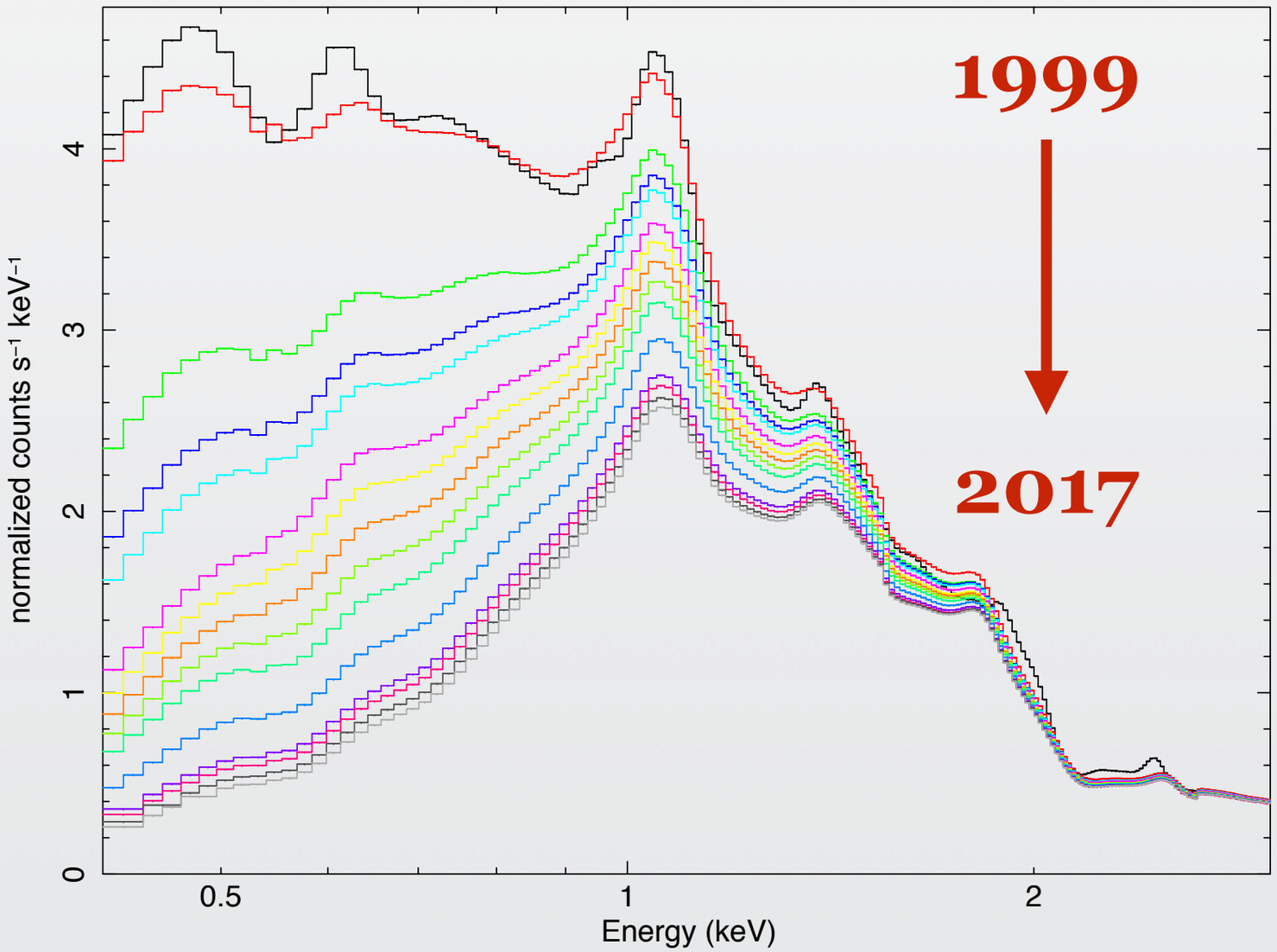

Monitoring the contaminant

Multi-prong approach to monitor the buildup of the contaminant

- Abell 1795
  - time dependence
  - spatial structure
  - covers ACIS-S and ACIS-I
- Blazars (e.g. Mkn 421)
  - time dependence
  - spatial structure
  - chemical composition
  - covers ACIS-S
- E0102
  - independent verification of contamination models
- ECS data
  - time dependence
  - spatial structure
  - covers ACIS-S and ACIS-I
  - fading due to its 2.7 years half-life

Monitoring the contaminant

Multi-prong attack to monitor the buildup of the contaminant

- **Abell 1795**
  - **time dependence**
  - **spatial structure**
  - **covers ACIS-S and ACIS-I**
- Blazars (e.g. Mkn 421)
  - time dependence
  - spatial structure
  - chemical composition
  - covers ACIS-I
- E0102
  - independent verification of contamination models
- **ECS data**
  - **time dependence**
  - **spatial structure**
  - **covers ACIS-S and ACIS-I**
  - **fading due to its 2.7 years half-life**

ACIS observations of A1795

- Raster scan with ACIS-S and ACIS-I once every year
- 3 pointings with ACIS-S
- 8 pointings with ACIS-I (alternated)
- Monitor the aimpoint every 6 months

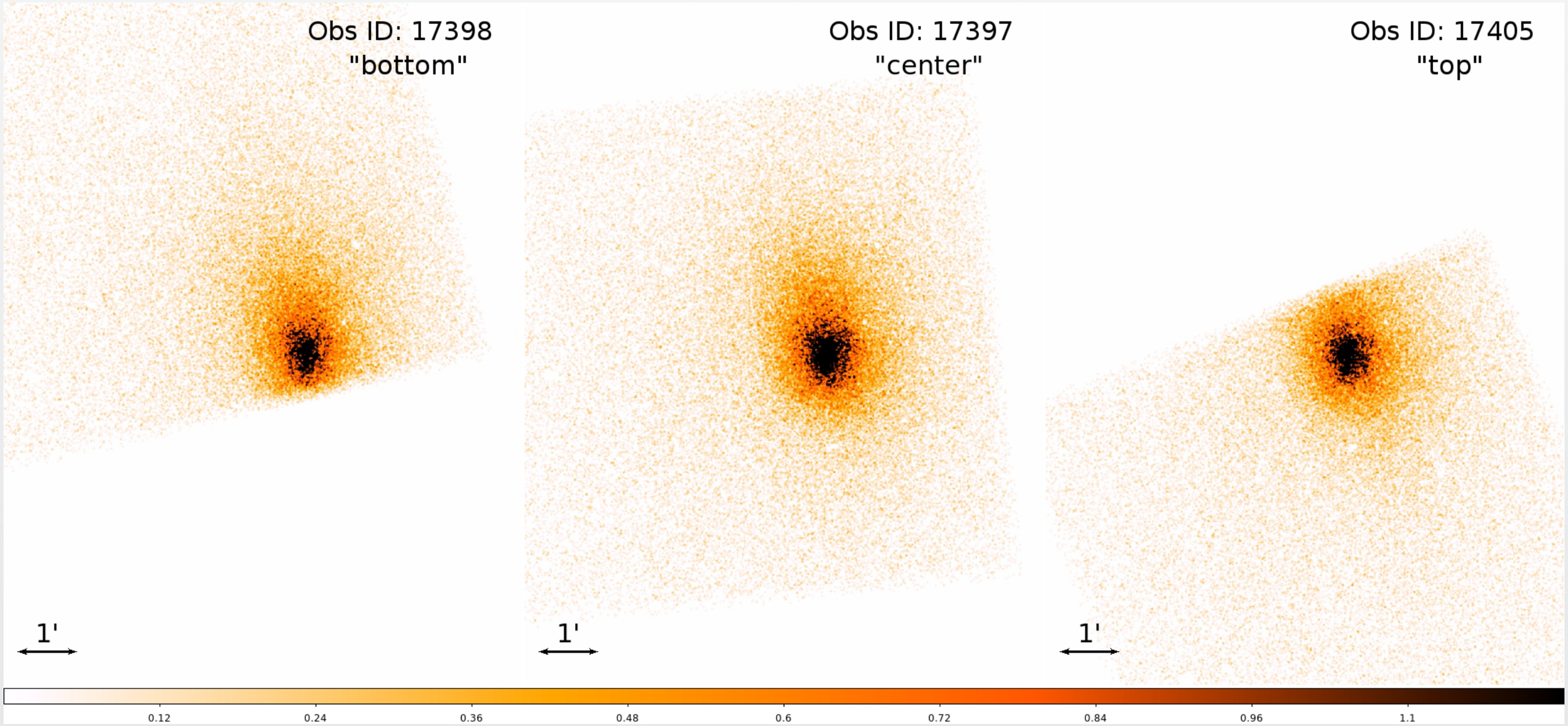

ACIS-I observations of A1795

- Raster scan with ACIS-S and ACIS-I once every year
- 3 pointings with ACIS-S
- 8 pointings with ACIS-I (alternated)
- Monitor the aimpoint every 6 months

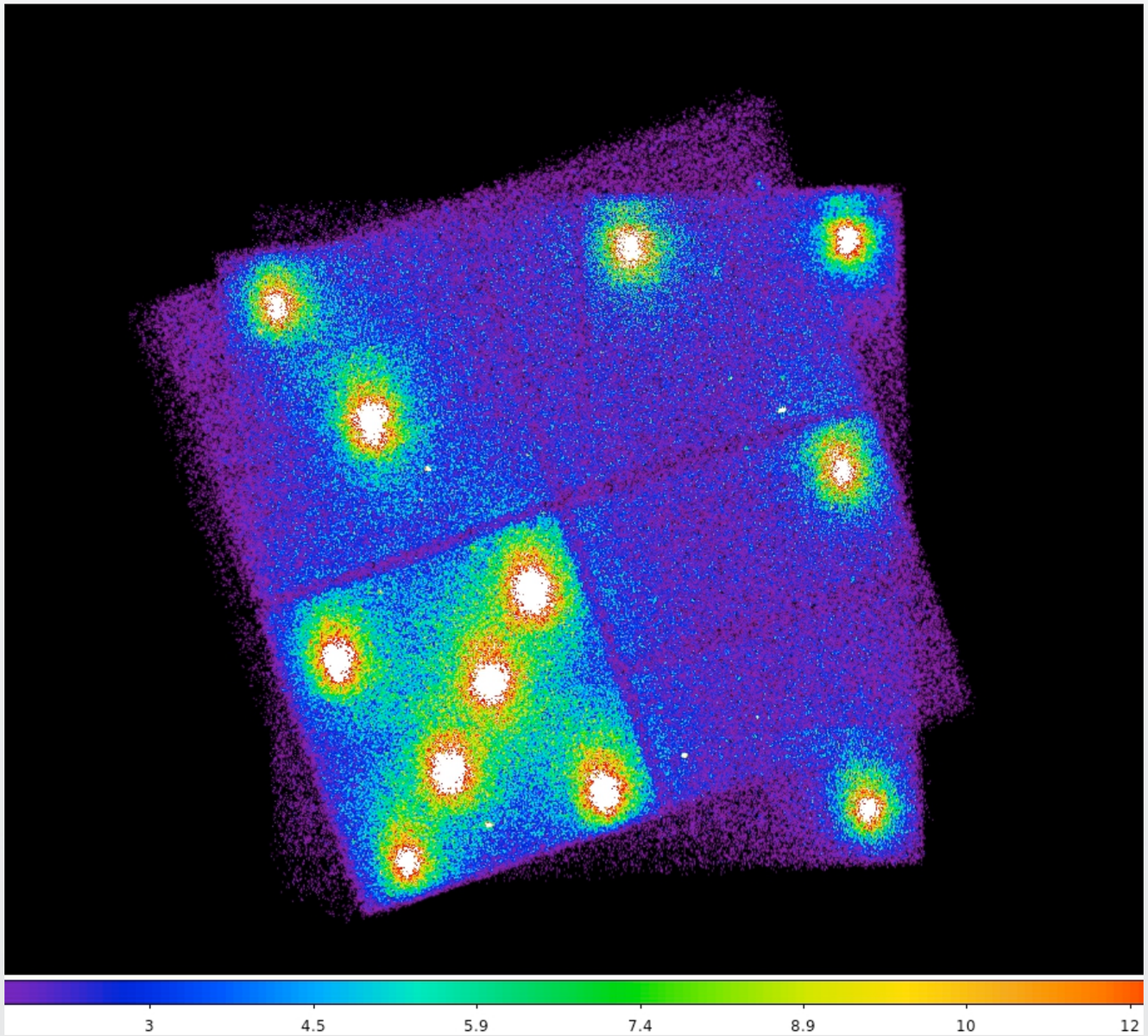

Time dependence of the contaminant

- Each observation is 15-20 ks
- Uniform data analysis procedure

- Computing the time dependence:
  - point sources excluded
  - spectral characteristics of Obs ID 494 (December 1999) used as reference by extracting circular region with 65” radius centered on A1795
  - spectrum described with Galactic column density, APEC models, and ACIS contamination with fixed O/C and F/C ratios
  - For subsequent observations the spectra of the same 65” circular region is extracted with the contamination correction turned off
  - The follow-up spectra are fit with best fit spectrum obtained from Obs ID 494 and additional ACIS contamination

Time dependence of contaminant in the center of ACIS-S

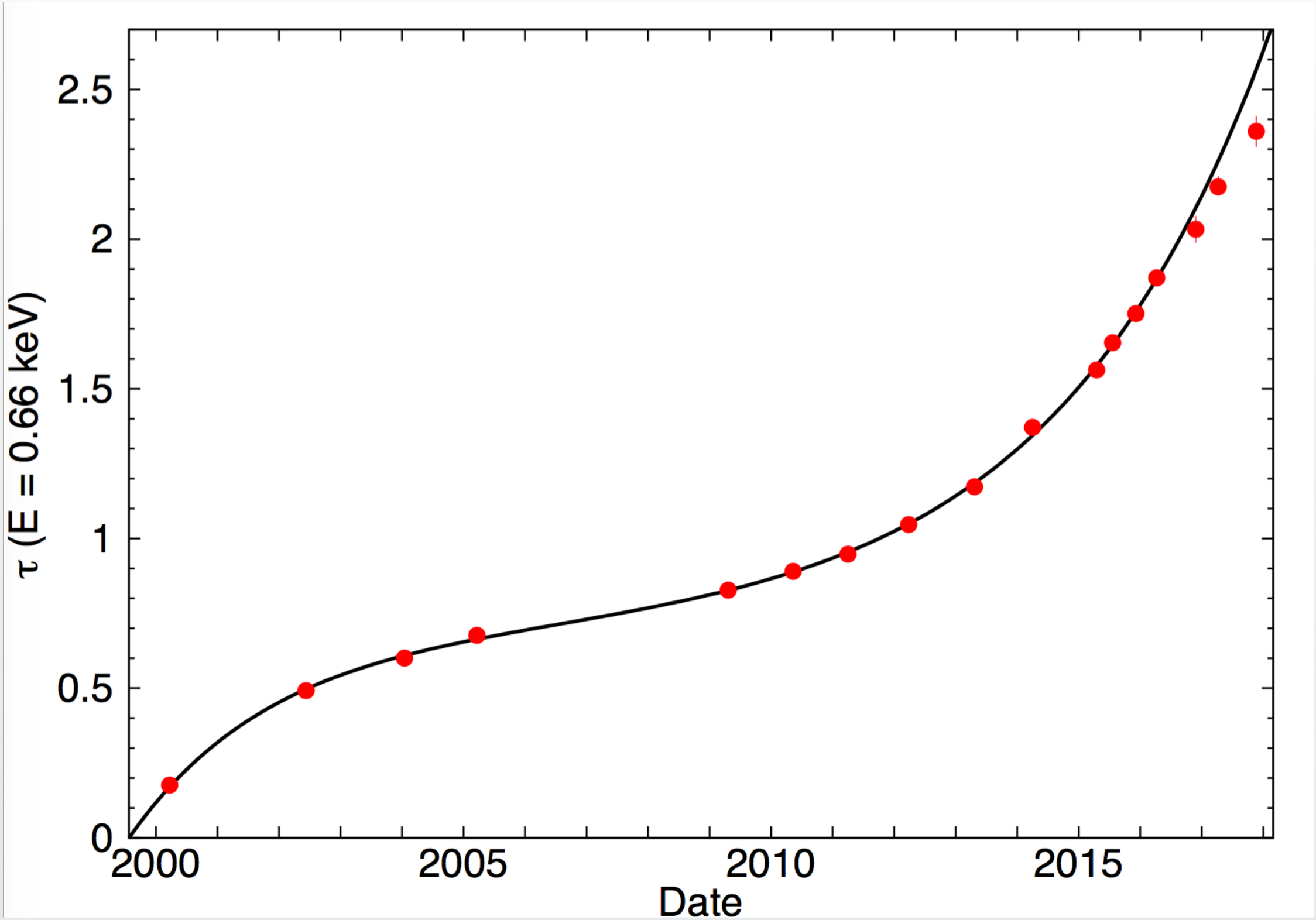

Time dependence of contaminant in the center of ACIS-I

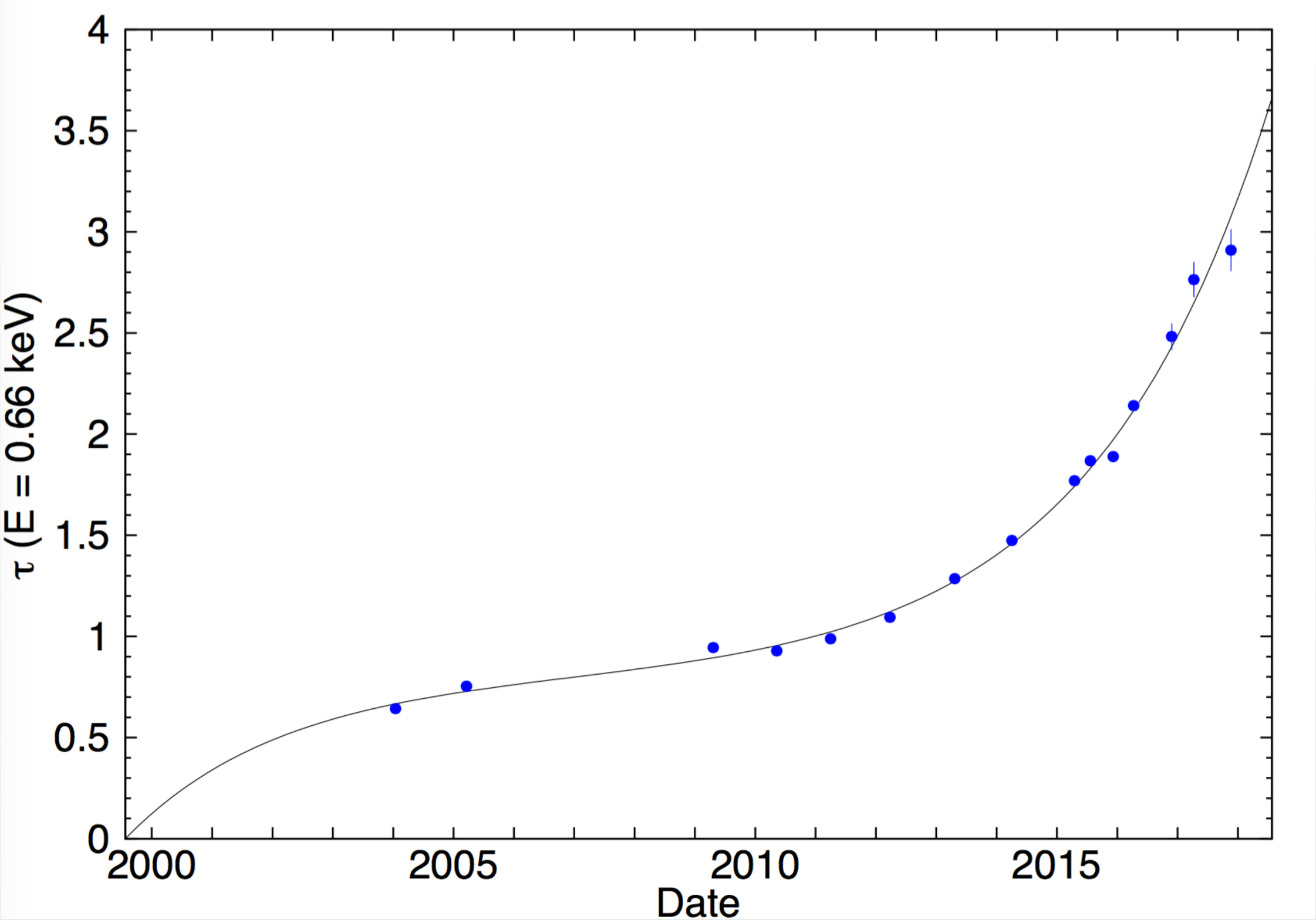

Conclusions on the time dependence of the contaminant in the center

- Accumulation of the molecular contamination on the OBF continues
- Although ACIS-S and ACIS-I had similar optical depths until about 2012, more recently ACIS-I appears to have higher contaminant level
- Rate of the buildup is slower than predicted based on the contamination model — new model to be released

Spatial structure of the contaminant

- Each observation is 20-25 ks
- Uniform data analysis procedure

- Computing the shape of the spatial structure:
  - point sources excluded
  - for each epoch a grid is defined centered on the center of A1795 extending along y direction of the detector
  - Spectra for each regions is extracted and ARFs are generated with the contamination correction turned off
  - For regions in the top/bottom chipy regions the extra contamination relative to the center is determined by extracting the spectrum in the same region and adding an extra contamination component
  - spectra are described with Galactic column density, single temperature APEC model, and ACIS contamination models with fixed O/C and F/C ratios

Spatial structure of the contaminant

- Raster scan with ACIS-S and ACIS-I once every year
- 3 pointings with ACIS-S
- 8 pointings with ACIS-I

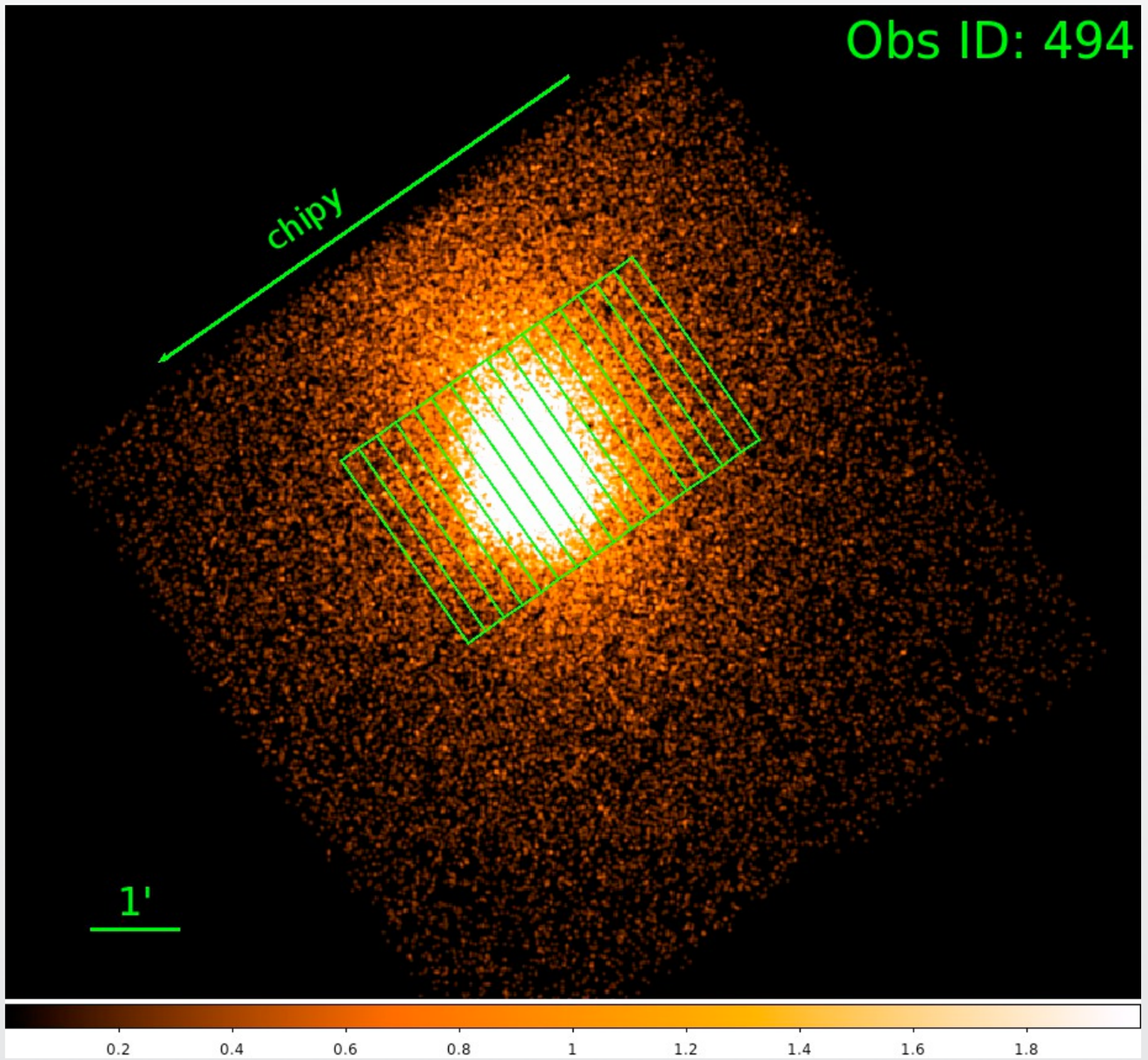

Shape of the spatial structure of the contaminant on ACIS-S

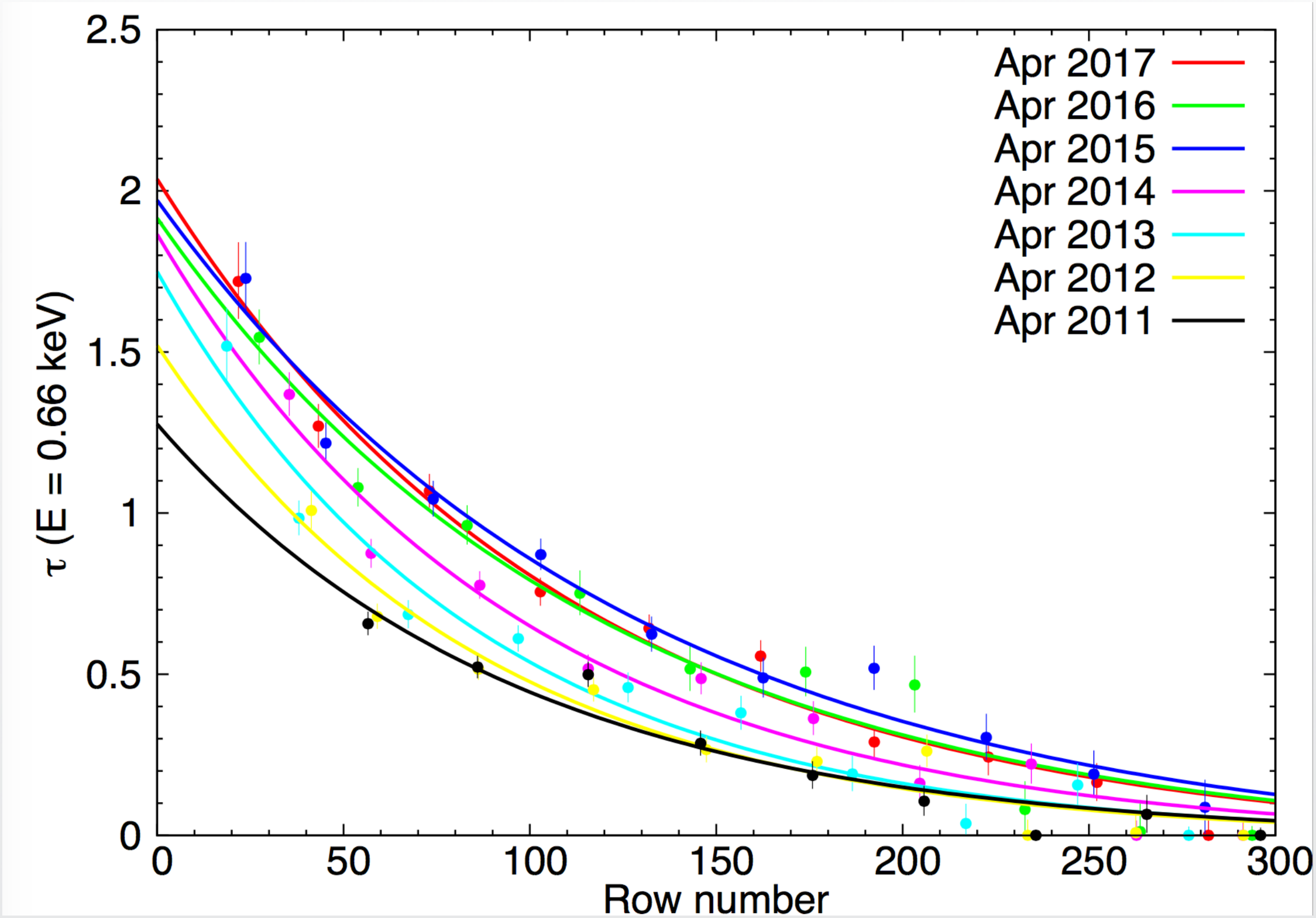

Edge-to-center difference using A1795 data

- Optical depth at y=64 relative to the center at E=0.66 keV
- ECS data up to 2008
- ACIS-S3 of Abell 1795 beyond 2008

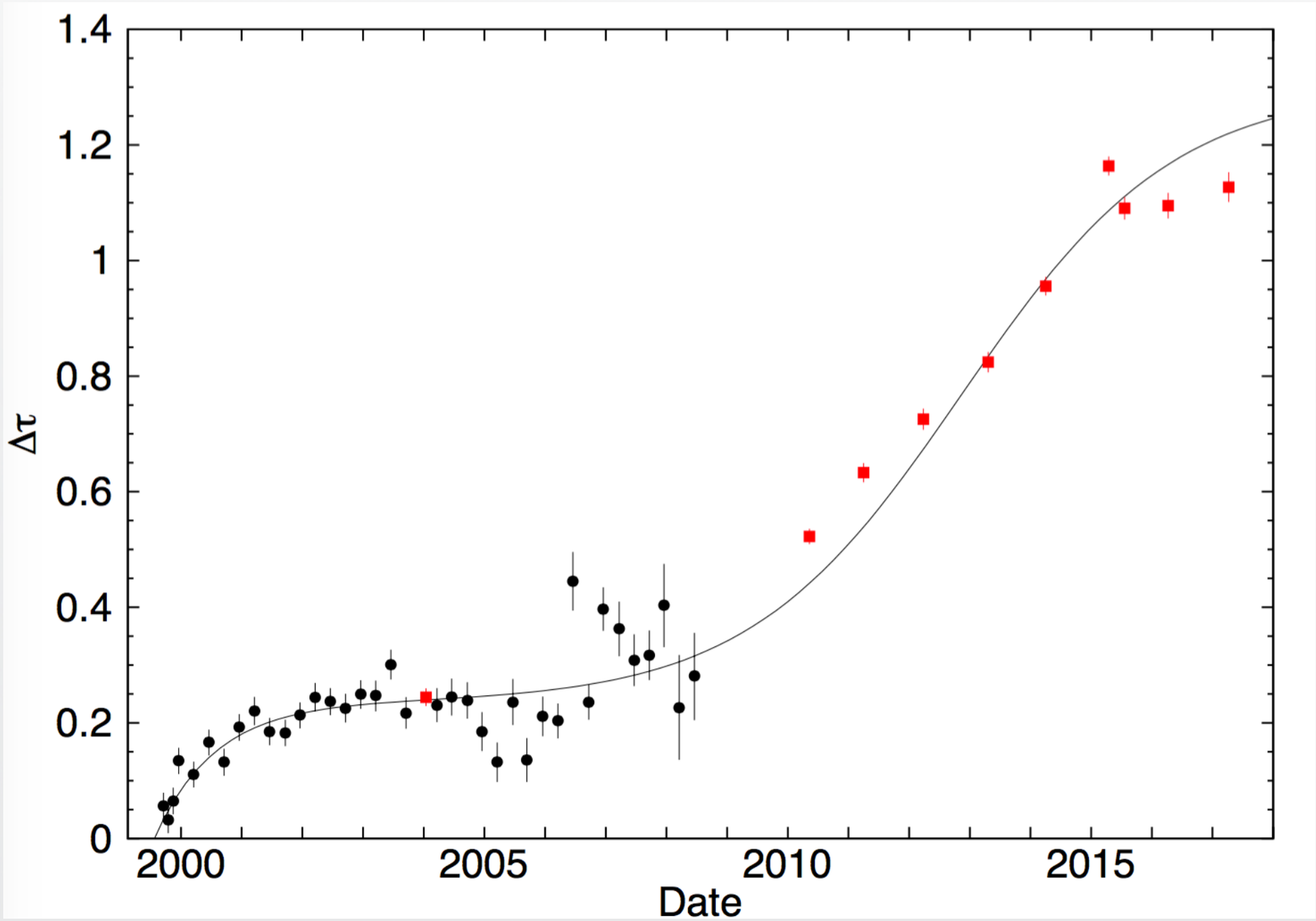

ECS observations

- ECS data can be used to measure the contaminant on the OBF
- Measure flux ratio of the L-complex to Mn-Kα lines
- Convert $f_L/f_{Mn\text{-}K\alpha}$ ratio to optical depth

L-complex

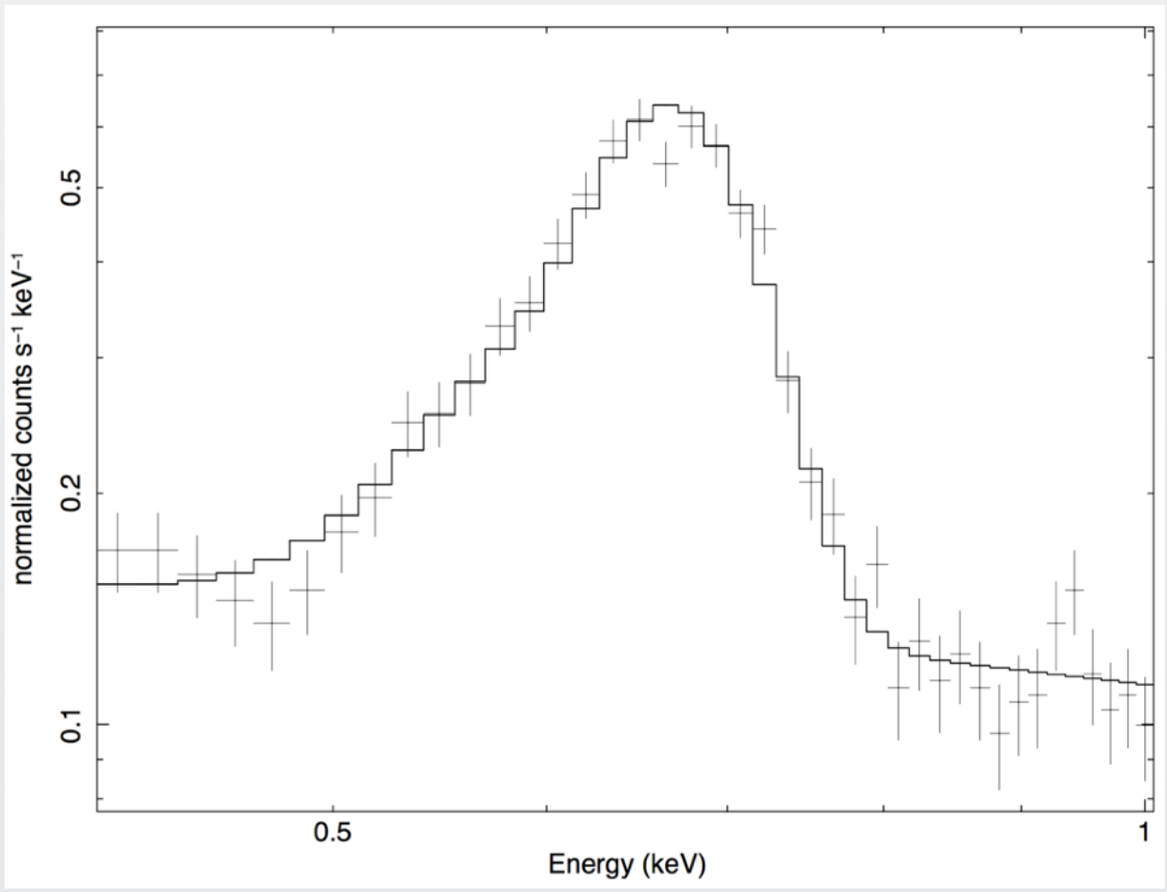

Al-Kα line Mn-Kα line

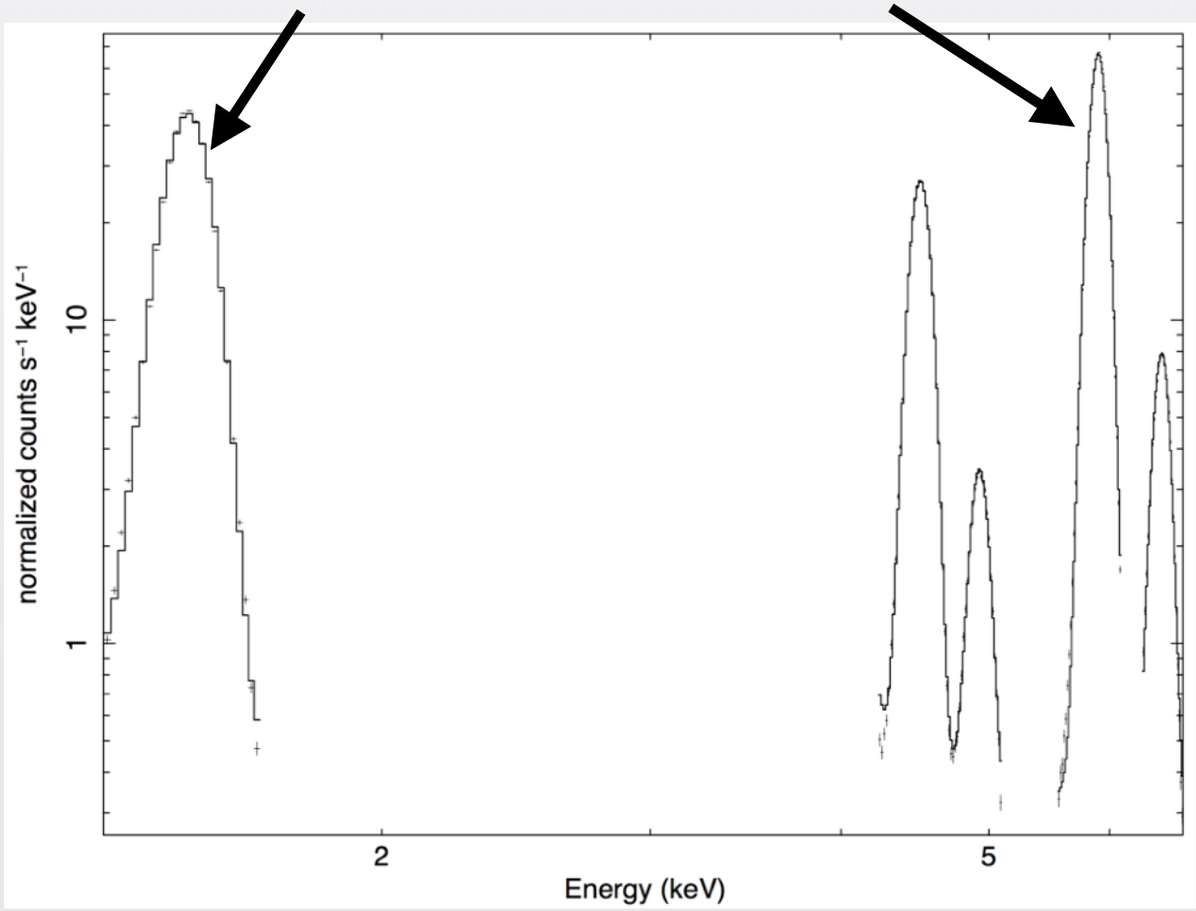

Edge-to-center difference using A1795 data

- Optical depth relative to the center at E=0.66 keV
- ECS data up to 2008
- ACIS-S3 of Abell 1795 beyond 2008

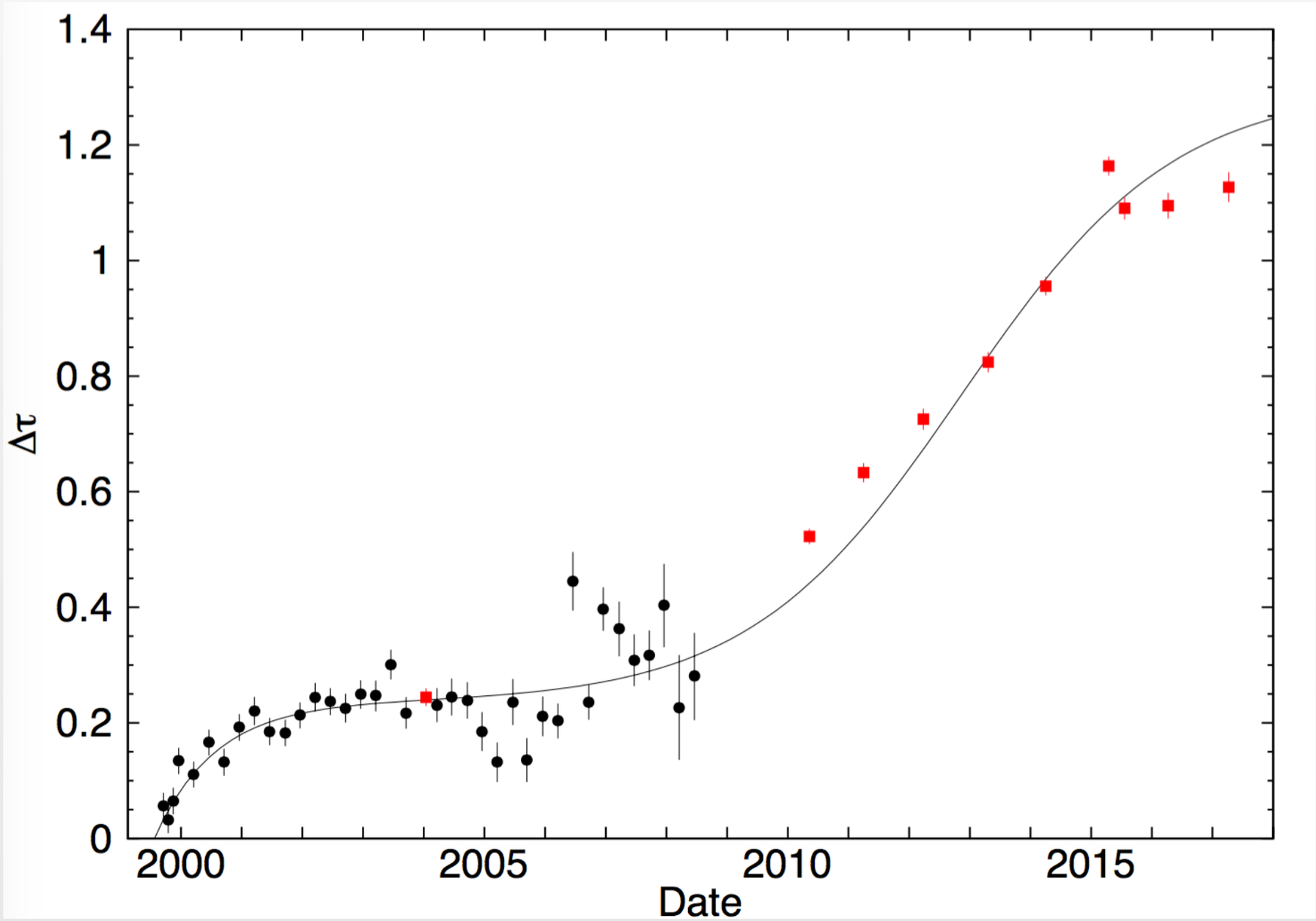

Weakening L-complex in S3

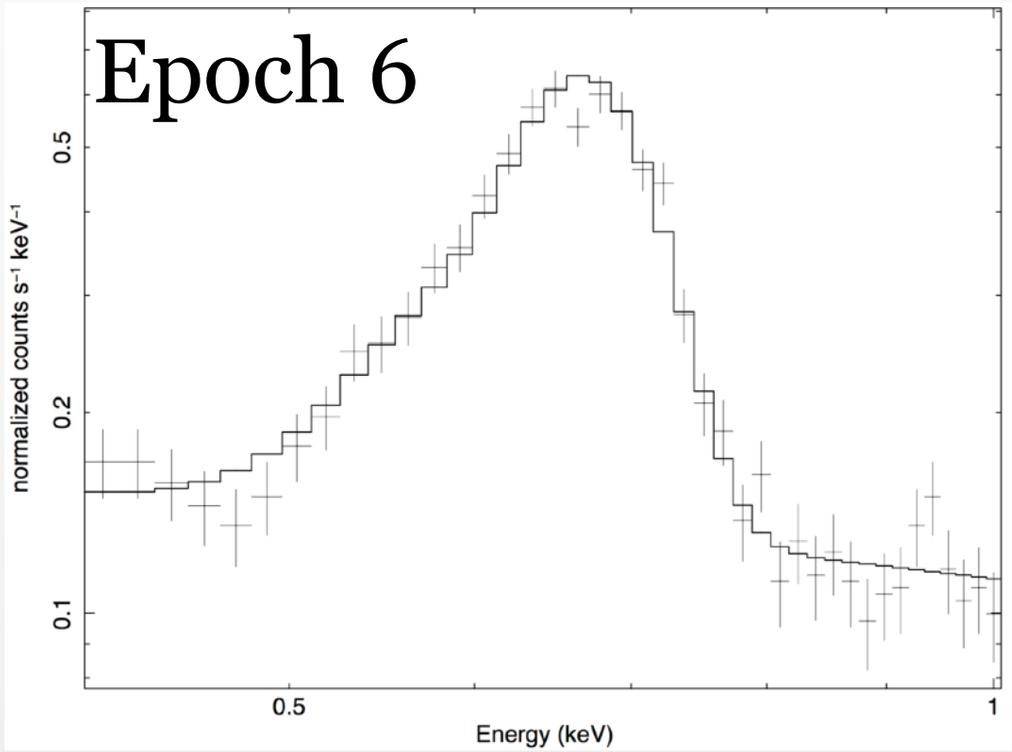

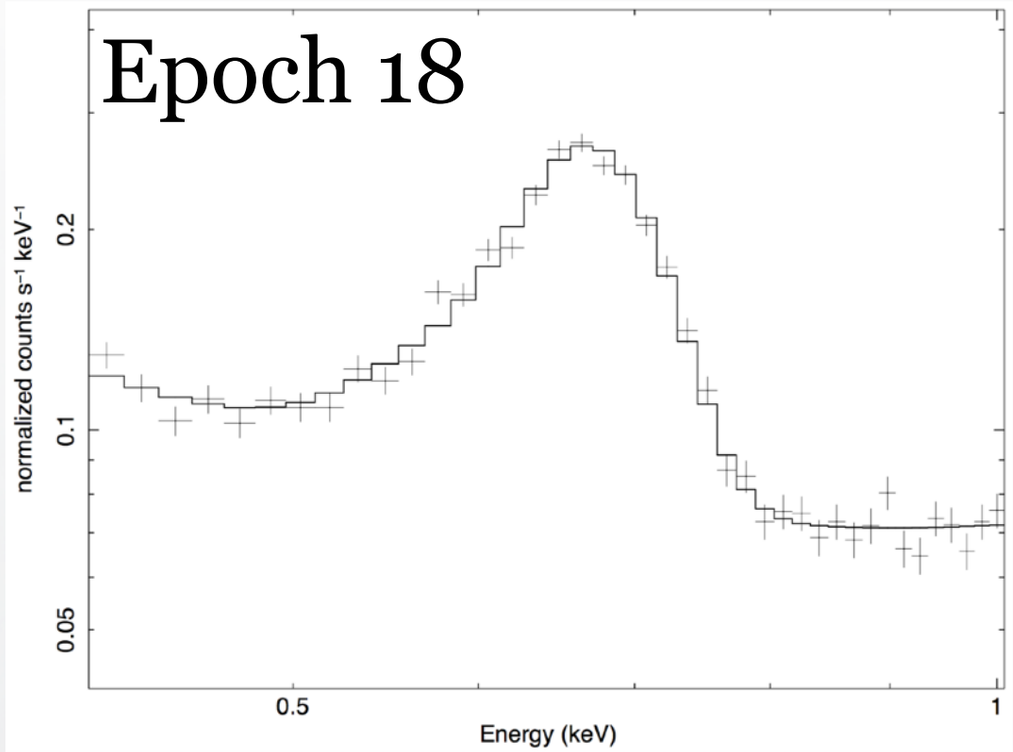

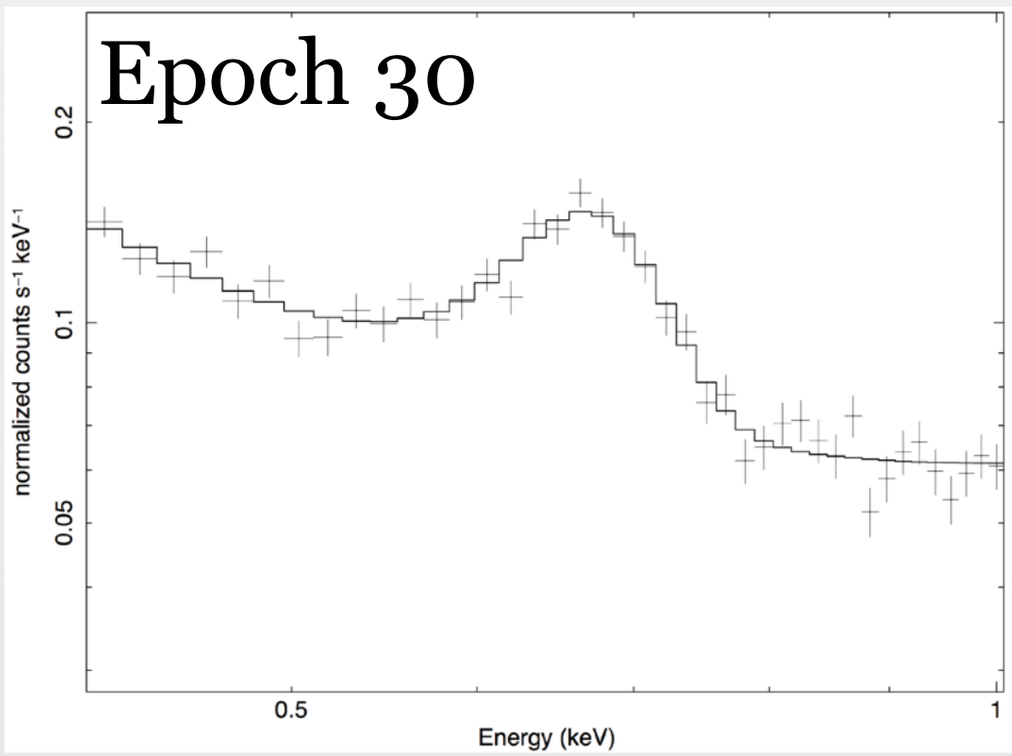

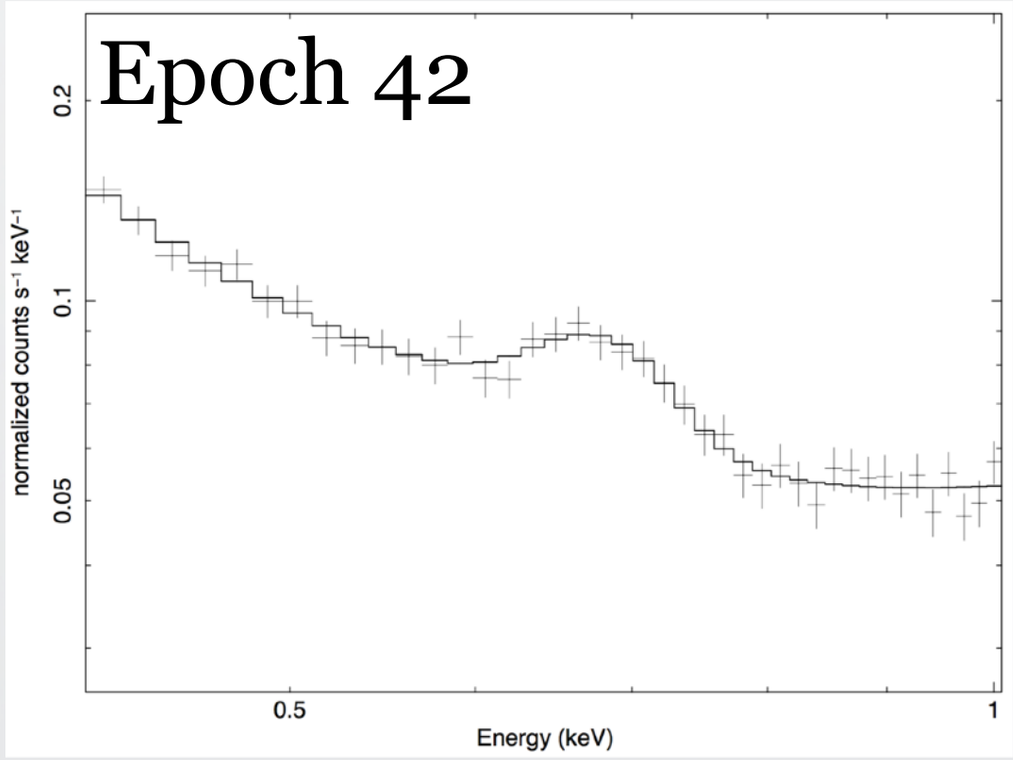

Al-Kα can be used to study the contamination

- Flux in L-complex decreases, statistical and systematic uncertainty increase
- After ~2005 L-complex cannot be used to compute accurate (<5%) optical depths

- However Al-Kα and Mn-Kα is strong and can be used to measure optical depths

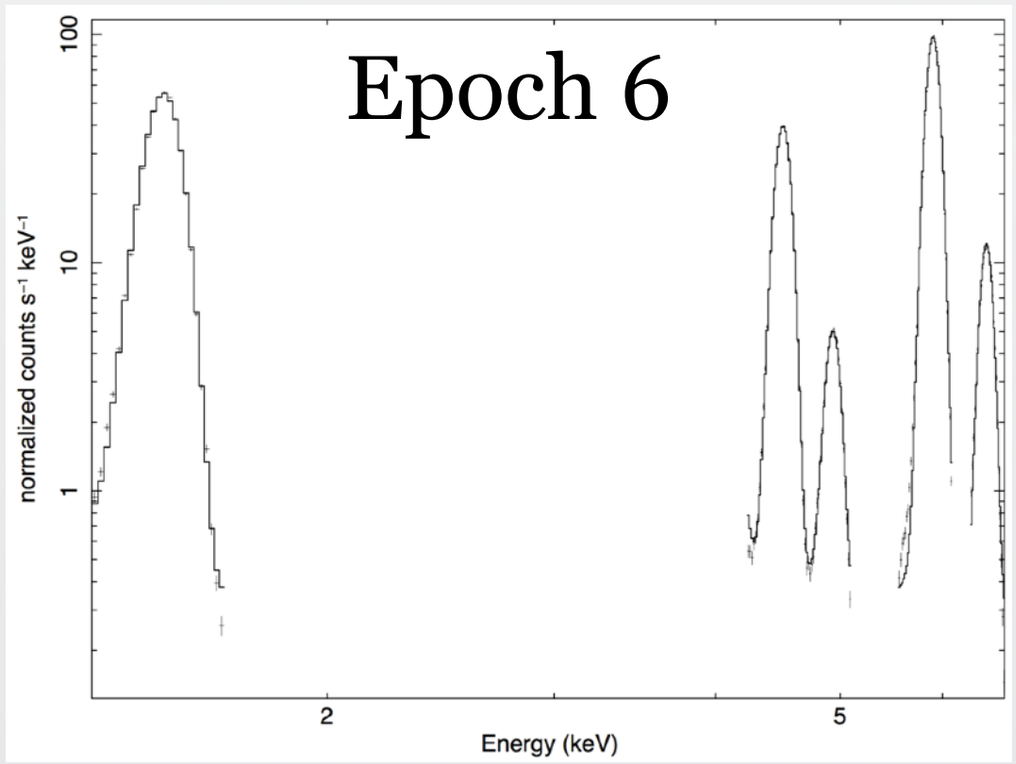

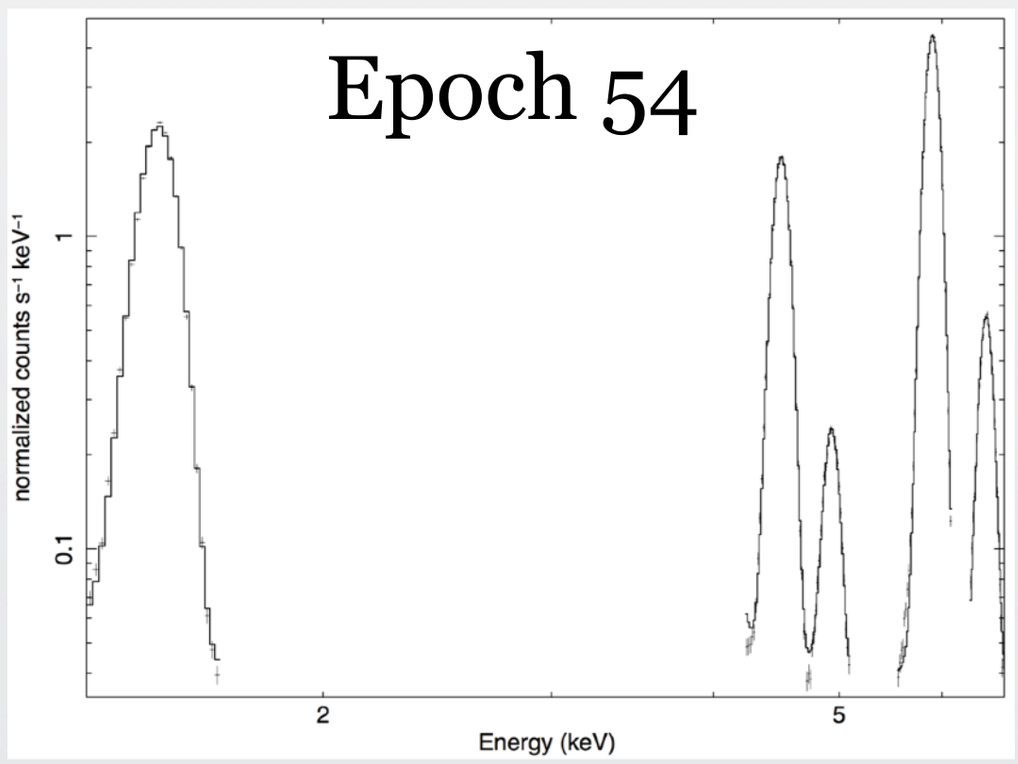

Evolution of the contaminant using ECS data

- Ratio of Al Kα to Mn Kα line is used to derive the optical depths
- Plot shows evolution of the optical depths at the center at E=1.49 keV

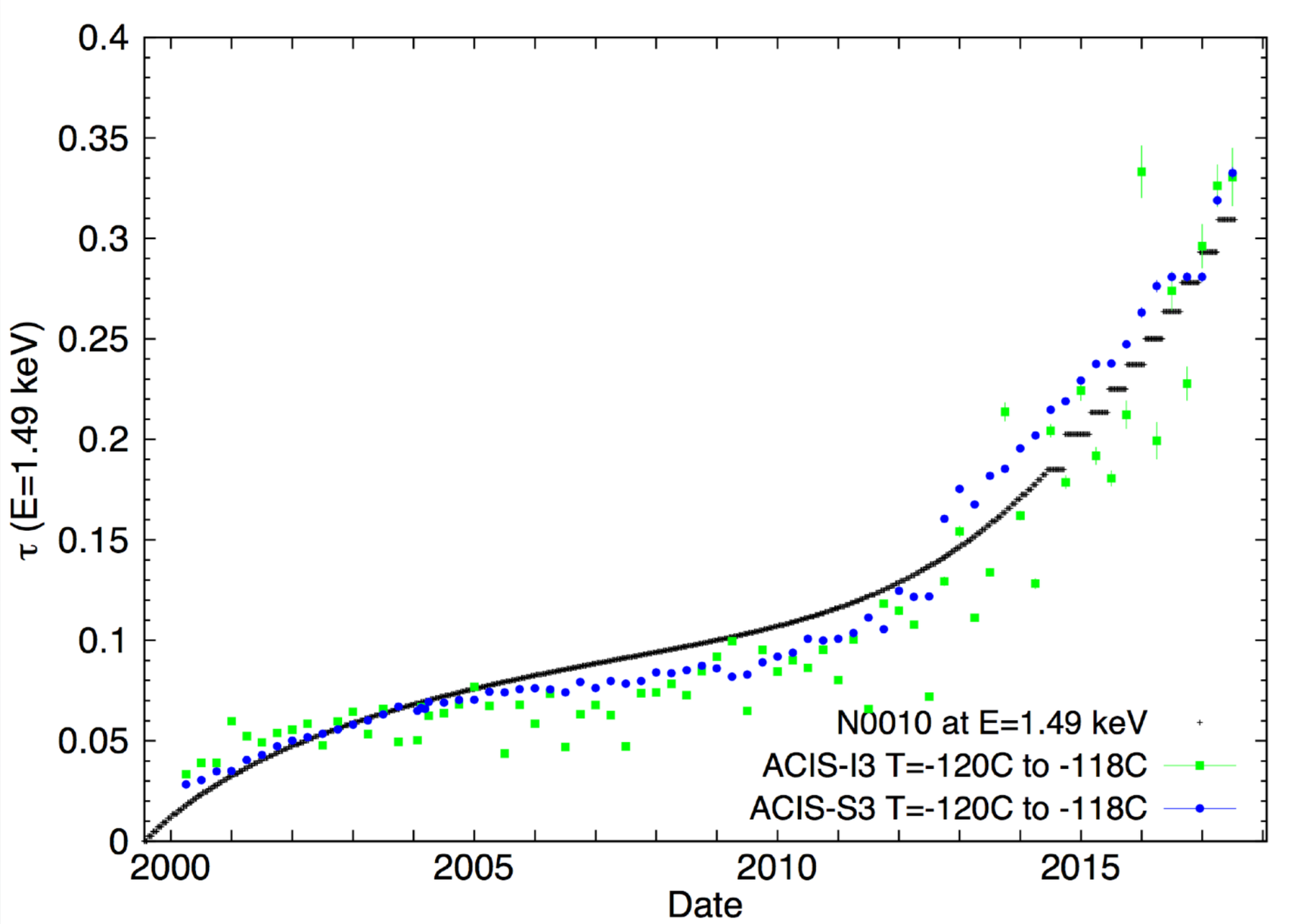

Edge-to-center difference using ECS data

- Ratio of Al Kα to Mn Kα line is used to derive the optical depths
- Plot shows optical depths relative to the center at E=1.49 keV

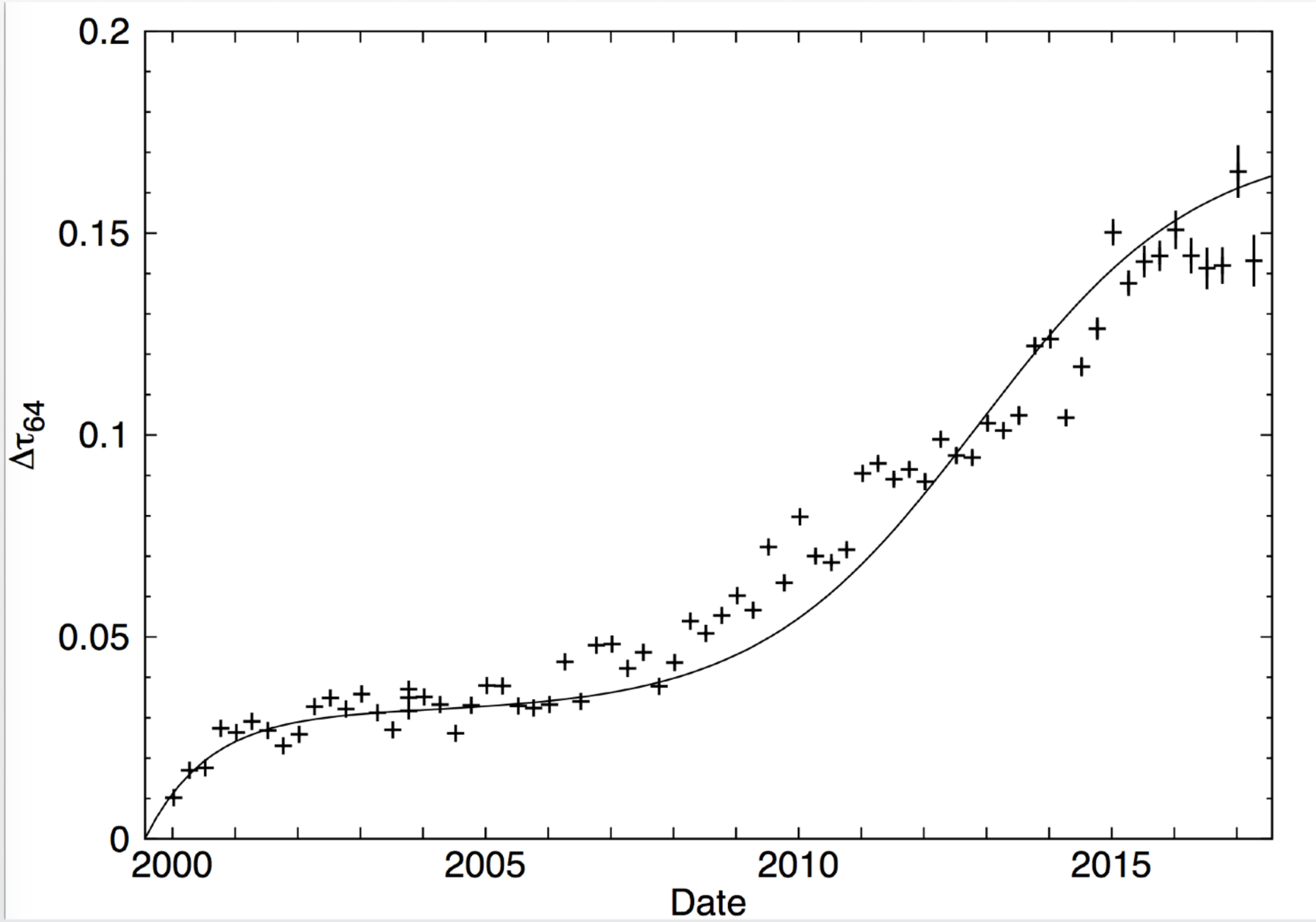

Conclusions on the spatial structure of the contaminant

1. The spatial structure of the contaminant can be described with an exponential model that is similar albeit slightly broader than before 2014
2. After the rapid increase in the center-to-edge difference between ~2009-2014, $\Delta\tau$ appears to level off
3. Another contaminant layer is accumulating that is less sensitive to temperature differences between the center and edge of the detector
4. ECS data (E=1.49 keV) is used to characterize the contaminant